Spanish Journal of Agricultural Research
19 (1), e0204, 10 pages (2021)
eISSN: 2171-9292
https://doi.org/10.5424/sjar/2021191-15884
Instituto Nacional de Investigación y Tecnología Agraria y Alimentaria (INIA)

RESEARCH ARTICLE

OPEN ACCESS

Development of a vibrationless sorting system

Selcuk Ugurluay[1] and Ibrahim Deniz Akcali[2]

[1] *Hatay Mustafa Kemal University, Faculty of Agriculture, Dept. of Biosystems Eng., Hatay, Turkey* [2] *Cukurova University, Faculty of Engineering and Architecture, Mechanical Eng. Dept., Adana, Turkey*

Abstract

Aim of study: Size classification is essential in many industrial processes. Most classical sorting systems use vibrations as a means of classification function. In this study, a vibration-free sorting system called helical cylindrical screen has been developed against the disadvantages of vibrating systems and proposed to be used in the sorting of crop seeds.

Area of study: Adana City, Turkey.

Material and methods: The movement of the seed mass on the screen surface was formulated and the mass movement along the circular-helical paths was analytically expressed, leading to some operational parameters for evaluation in the screen design. By combining the mass movement parameters with effective separation conditions, an algorithm was obtained against the desired mass flow rate to determine the appropriate values of the design parameters. Experiments were performed on the machine, which was manufactured to sort peanut seeds into two different sizes, small and large.

Main results: The results obtained in the experiments (separation efficiency, mass flow rate, effect of grain size on separation efficiency and equilibrium angle) were compared with the theoretical ones. The separation efficiency of the machine (99% and above) was quite good and is not affected at all by the small size ratio contained in the mixtures. The limitations of the theoretical velocities (axis and tangent) of a seed moving on the cylindrical sieve were found to be consistent with those obtained experimentally.

Research highlights: The helical cylindrical sieve can be used for other particulate agricultural products with smooth surfaces such as soybeans, kidney beans, peas, etc.

Additional key words: cylindrical helical screen; efficiency; equilibrium angle; screening conditions; size sorting.

Authors' contributions: Conceived and designed the experiments, performed the experiments, wrote the paper: SU, IDA. Critical revision of the manuscript for important intellectual content: IDA. Statistical analysis: SU.

Citation: Ugurluay, S; Akcali, ID (2021). Development of a vibrationless sorting system. Spanish Journal of Agricultural Research, Volume 19, Issue 1, e0204. https://doi.org/10.5424/sjar/2021191-15884

Received: 16 Oct 2019. **Accepted:** 25 Mar 2021.

Funding: The authors received no specific funding for this work.

Competing interests: The authors have declared that no competing interests exist.

Correspondence should be addressed to Selcuk Ugurluay: ugurluay@mku.edu.tr; ugurluay@hotmail.com

Introduction

Sorting, the separation of granular material into one or more fractions on the basis of some measurable physical property, is required in many industrial processes including the preparing of foods (Feistritzer *et al.*, 1981; Fellows, 2000; Grandison, 2006). Size sorting, in which separation process is based on the measurable physical property being size, is physically and most economically realized by means of vibrating systems. Vibrating systems realizing the separation function involve vibrating screens. There are works in the literature in which different aspects of vibrating screens have been handled. Tan & Harrison (1987) have investigated the influence of several different planar and spatial drive mechanisms on the screening efficiency by means of the so called screening index. Shen *et al.* (2009) reported a novel vibration sieve mechanism based on a parallel mechanism, in which optimum design has been demonstrated with regard to structure, kinematic analysis and motion simulation. The motion of granular material has also been analyzed by Hongchang & Yaoming (2011) with respect to a performance parameter called throwing index, the most suitable value of which has been found corresponding to the best performance of vibrating screen.

The vibrating screen has found extensive applications in many different areas. For instance, in coal processing, vibrating screen with variable elliptical trace has been examined from the standpoint of its "ideal motion" with the purpose of improving processing capacity and efficiency through computer models (He & Liu, 2009). In the area of construction bulk material screening for civil engineering purposes, sieve vibrations have been analyzed by another work utilizing computer models involving an

algorithm based on the so-called false-position method (Stoicovici *et al.*, 2009). There have been some works related to the vibratory motion of the granular material using the so-called Discrete Element Method (DEM). For instance, Alkhaldi & Eberhard (2006) have analyzed screening phenomena in mechanical environment called vertical tumbling cylinder. A numerical study of the motion particulates along a circularly vibrating screen deck has been done using the three - dimensional DEM (Zhao *et al.*, 2011) in which the effect of vibration amplitude, throwing index and screen deck inclination angle on the screening process has been determined for optimizing the design of screen separators.

A number of disadvantages associated with vibrating screens can be stated. In the first place, accelerations are unavoidable part of vibrating screens. This means large inertia forces in connection with large moving masses. These inertia forces do not only raise power consumption but also create material fatigue stresses. Vibrations cause at the same time disassembling forces on the connections. Additionally, unbearable noise levels are the results of vibrations.

Jiannan *et al.* (2017) developed and used rotary table-roller coating equipment to coat peanut seeds. Inspired by such studies and due to the above mentioned negative aspects of vibrating sieves, the idea of using cylindrical sieves has been formed in the classification of seeds.

In this study, a rotary cylindrical screen was designed based on the idea that sieving and grading processes can be performed without vibration. To ensure control and continuity over the flow of the sorting material, helicoid surfaces were placed inside the cylindrical screen. In order to free the motion of the sorting material off vibrations to induce a uniform flow, the screen was rotated at a constant speed. The movement of the kernels was modeled on the basis of a continuous layer of particles directed along circular and helical paths. Finally, the theoretical classification conditions were compared with the results obtained in the experiments.

Material and methods

Theory

Based on the fact that one significant factor in causing inefficiency in the sorting of particulate material is the uncontrolled, irregular motion of the particulate material relative to the mechanical medium by which sorting is to be realized. Thus, in order for the efficiency of sorting to be improved, there is a need to regulate the motion of the material. To this end, the motion of the particulate material is considered to be regulated in two ways. The first one is to understand and formulate the motion of the material in a rotating cylinder and the second one is the understanding and formulating how this circular motion is affected by a helicoid wrapped inside the cylindrical surface.

In order to formulate the motion of the material Fig. 1a is considered. The basic assumptions in this formulation were that there is a single and continuous layer of average thickness of "e" supposed to slide only, excluding any rolling or tumbling motions. Practical means can be deployed to satisfy these assumptions (Fig. 1b). The cylinder which receives particulate material from the feeder is rotating at an appropriate constant speed w and has a radius of r. The coefficient of friction between surface of the cylinder and the granular material is μd. As the cylinder rotates, the particulate material assumes a height from the lowest point of the cylinder which means a gain of potential energy. Under suitable motion conditions this potential energy will be converted into a relative sliding motion of the particulate material with respect to the surface of the cylinder. Then the material inside the rotating cylinder will come to equilibrium under the influence

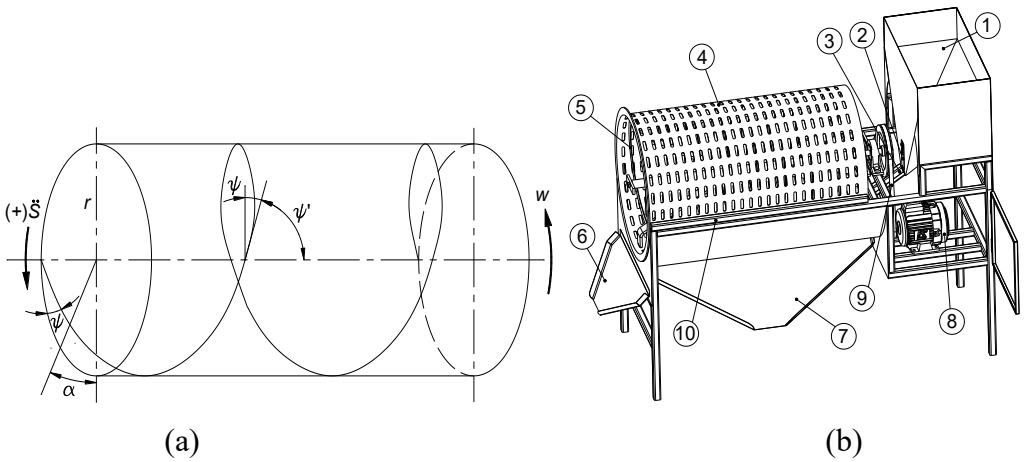

Figure 1. Helical path in the screen (a) and the prototype sorting machine (b): 1, store; 2, feeder outlet; 3, transport channel; 4, cylindrical sieve; 5, helical paths; 6, large kernels output; 7, small kernels output; 8, electrical motor; 9, belt pulley mechanism; 10, brush.

of basically three forces, which are particulate material weight, friction force and inertial force.

Now, the equilibrium position of the layer of particulate material will be formulated referring to Fig. 2. In Fig. 2 an infinitesimal mass (*dm*) of layer of particulate material is considered at a position of α from the vertical axis, which is assumed to come to equilibrium under the influence of static weight (*dm.g*), where g represents gravitational acceleration, inertial force (*dm.w2.r*), interaction force (*Nr*) between the infinitesimal mass and internal cylinder surface and friction force (*μd.Nr*), F force representing resistive effect of the rest of the layer below α position, *F+dF* representing the force responsible for the downward sliding motion, where *dF* is a force change due to a position change dα.

If equilibrium equation along the surface normal of the cylinder is considered, assuming outward to be positive the following equation is written:

$$-N_r + dm.w^2.r + dm.g.cos\alpha = 0 \qquad (1)$$

Now, assuming downward sliding direction to be positive, equilibrium equation is written along the sliding direction:

$$dF - \mu.N_r + dm.g.sin\alpha = 0 \qquad (2)$$

If the interaction force *Nr* is drawn from Eqn. (1) and substituted in to Eqn. (2) the following results:

$$dF = dm[-g.sin\alpha + \mu(w^2.r + g.cos\alpha)] \qquad (3)$$

Now designating the thickness of the particulate layer by *e* and layer density per unit length by *ρ*, infinitesimal mass *dm* can be expressed as follows (Fig. 2):

$$dm = \rho.r.e.d\alpha \qquad (4)$$

Substituting dm from Eqn. (4) into Eqn. (3) and integrating between α_0 and β, where α_0, β designate the angular position of the beginning and end of the layer, respectively, the following is obtained:

$$F(\alpha_0,\beta) = g(-cos\alpha_0 + cos\beta) + \mu_d.g(sin\beta - sin\alpha_0) + \mu_d.w^2.r(\beta - \alpha_0) = 0 \qquad (5)$$

By Eqn. (5) it becomes possible to estimate the span (β-α_0) of the layer which comes to equilibrium during the rotation of the cylinder. If α_0 is assumed to be 0, meaning that the layer starts from the lowest position, Eqn. (5) turns out to be:

$$F(\beta) = g(-1 + cos\beta) + \mu_d.g.sin\beta + \mu_d.w^2.r.\beta = 0 \qquad (6)$$

The importance of F function described by Eqns. (5) and (6) lies in the fact that it represents the net force acting on the layer along the motion direction, which is necessarily zero for equilibrium under stable steady-state conditions.

Eqn. (6) is a nonlinear algebraic equation in the unknown β which requires numerical solution. Nevertheless, for small β angle an initial solution to start a numerical iteration procedure can be found as follows:

$$sin\beta \approx \beta \qquad \text{or} \qquad cos\beta \approx 1 - {\beta^2}/{2} \qquad (7)$$

$$\left(\frac{\beta^2}{2}\right) - \mu_d.\beta\left(1 + \frac{w^2.r}{g}\right) = 0 \qquad (8)$$

$$\beta_1 = 0, \qquad \beta_2 = 2\mu_d\left(1 + \frac{w^2.r}{g}\right) \qquad (9)$$

In order to determine the location (θ*) of the center of gravity of the layer, it is necessary to take into account the external moment about cylinder axis that will cause the mass *dm* to have a potential energy of *dm.g.r*(*1-cos* α). Accordingly the center of mass is determined as follows;

$$sin\theta^* = \frac{\int_{\alpha_0}^{\beta}(dm.g)r.sin\alpha}{r\int_{\alpha_0}^{\beta} dm.g} \qquad (10)$$

Substituting relationship (4) in Eqn. (10) and carrying out integration, the following is obtained:

$$sin\theta^* = \frac{(cos\alpha_0 - cos\beta)}{\beta - \alpha_0} \qquad (11)$$

If α_0 is assumed to be 0, meaning that the layer starts from the lowest position, Eqn. (11) becomes:

$$sin\theta^* = \frac{(1 - cos\beta)}{\beta} \qquad (12)$$

The significance of the center of mass lies in the fact that the whole layer of particulate can be imagined to be concentrated as a lumped mass at that point so that the motion of the layer can be better understood. For small angles θ*, α_0 and β the following approximate relationship can be given:

$$\theta^* = \frac{\alpha_0 + \beta}{2} \qquad (13)$$

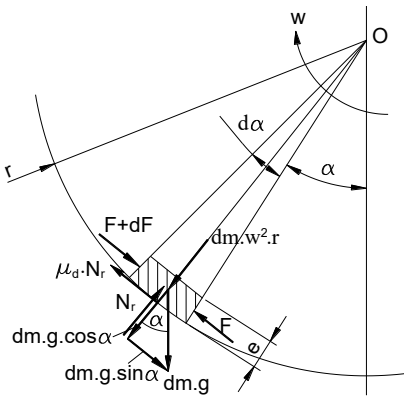

Figure 2. Forces acting on sliding mass (dm).

In particular when α_0 is set equal to 0 it can be shown that:

$$\theta^* \cong \frac{\beta}{2} \cong \mu_d(1 + \frac{w^2.r}{g}) \quad (14)$$

By means of Eqn. (14) it is possible to visualize the circular motion of the layer as such: when the layer center of mass exceeds θ^* value it means tendency to have sliding acceleration and when it comes to this angle the layer will assume equilibrium positon.

In order to let the layer of particulate material to be forwarded along the cylinder axis (Z-axis) a helicoid will be installed into its internal surface of the rotating cylinder. Now the motion of the layer along helical path will be described mathematically. The net force on the layer of mass *dm* downwards in a circular cross section is conceived to be *dm*.g.sinα at a positon of α. This force will be decomposed into axial force component of $dm.g.sin\alpha.cos\psi$ and normal force component of $dm.g.sin\alpha.sin\psi$ where ψ is the angle of helical path with the vertical direction (Fig. 3). Now equilibrium equations will be written along the radial, helicoid normal and helical sliding directions, respectively.

$$-N_r + dm.w^2.r + dm.g.cos\alpha = 0 \quad (15)$$

$$-N_h + dm.g.sin\alpha.sin\psi = 0 \quad (16)$$

$$dF + dm.g.sin\alpha.cos\psi - \mu_h.N_h - \mu_d.N_r = 0 \quad (17)$$

where N_h, μ_h are interaction force and coefficient of friction between helicoid surface and layer, respectively. If N_r and Nh are drawn from Eqns. (15) and (16) respectively together with Eqn. (4) substituted into Eqn. (17) and integration is carried out between β_0 and β_h, the following equation results:

$$G(\beta_0,\beta_h) = g(cos\beta_0 + cos\beta_h)(cos\psi - \mu_h.sin\psi) + \mu_d[g(sin\beta_h - sin\beta_0) + w^2.r(\beta_h - \beta_0)] = 0 \quad (18)$$

For a particular case of β_0=0, Eqn. (18) becomes:

$$G(\beta_h) = g(-1 + cos\beta_h)(cos\psi - \mu_h.sin\psi) + \mu_d(g.sin\beta_h + w^2.r.\beta_h) = 0 \quad (19)$$

Both Eqns. (18) and (19) signify net forces acting on the whole layer, which are 0 under equilibrium conditions. If for small angles in Eqn. (7) is used in Eqn. (19) the following relationships are obtained:

$$\beta_h = \frac{2.\mu_d}{(cos\psi - \mu_h.sin\psi)}(1 + \frac{w^2.r}{g}) \quad (20)$$

If equilibrium angles for circular and helical motions represented by Eqns. (9) and (20) respectively are compared, it will be seen that under the condition

$$0 < cos\psi - \mu_h.sin\psi < 1 \quad (21)$$

equilibrium angle (β_h) for helical motion will be greater than that (β) for circular motion. In order to estimate the mass flowrate (*dm/dt*) through the rotating cylinder, two elements are needed as depicted in Fig. 4.

$$\frac{dm}{dt} = \rho.A.v_z = \rho.r.e.\beta.v_z \quad (21)$$

where, from Fig 4-b

$$v_z = w.r.tan\psi \quad (22)$$

$$v_\theta = w.r \quad (23)$$

Conditions of screening

The basic principle underlying size sorting is that a particle of a particular size falls into the relevant section by passing through the holes of the screen. In order for the principle to be materialized, the control over particle velocity is essential. It is assumed that the holes are always open and ready to allow the passing of the particle without hindrance.

In order to derive the mathematical expressions related with the velocity control, a particle is shown in Fig. 5 at an initial position before entering the hole of the screen.

If Newton's Second Law is written for the motion of the particle in the z and y axes (Fig. 5), the following equations result:

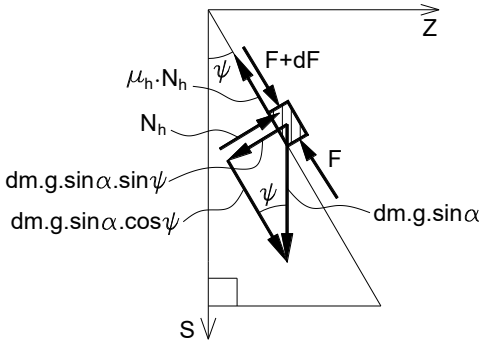

Figure 3. Forces on developed plane

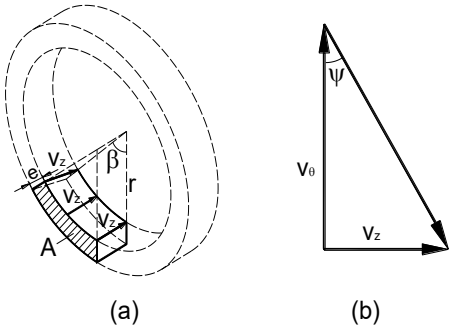

Figure 4. Mass flowrate formulation.

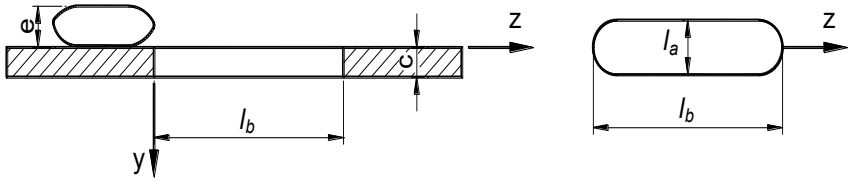

Figure 5. Motion of a single particle by the sieve hole

$$\frac{d^2z}{dt^2} = 0, \qquad \frac{d^2y}{dt^2} = g, \tag{24}$$

Assuming that the particle has velocity vz and zero displacement initially, the solutions of equation set (24) will be following:

$$z = v_z.t\,, \qquad y = \frac{1}{2}g.t^2 \tag{25}$$

In case t is eliminated in equation set (25), the following is obtained:

$$y = \frac{g.z^2}{2.v_z^2} \tag{26}$$

Now, the condition for the particle to pass through the hole without hitting its lower corner can be established as such:

$$y \geq c + e, \quad z = l_b \tag{27}$$

where, *c, e*, l_b are the sheet metal thickness, particle thickness, hole length, respectively. If conditions (27) are evaluated in Eqn. (26), the following result is obtained:

$$v_z = l_b\sqrt{\frac{g}{2(c+e)}} \tag{28}$$

It means that the particle velocity in the z direction should be restricted.

Similarly, by the same reasoning the tangential velocity (v_θ) in the direction perpendicular to cylinder axis should also be limited through the following relationship:

$$v_\theta = l_a\sqrt{\frac{g}{2(c+e)}} \tag{29}$$

where l_a is the width of hole.

Relationships (28) and (29) imply that the particle should have controlled velocities along the cylinder axis as well as perpendicular to it for effective screening.

Efficiency formulation

System efficiency (η) is formulated according to criteria of separating the input mass into two parts referred to as small-size group and large-size group as follows;

$$\eta = r_K.r'_K.\eta_K + r_B.r'_B.\eta_B \tag{30}$$

$$r_K = \frac{K}{K+B}, r_B = \frac{B}{K+B}, \; r'_K = \frac{K'}{K'} = 1, \; r'_B = \frac{B}{K_B+B}, \eta_K = \frac{K'}{K}, \; \eta_B = \frac{B'}{B} = 1 \tag{31}$$

where *K* is small-size group mass content, *B* is large-size group mass content of the inflowing mass, *K*' is the small-size mass content, K_B is small-size items mass content in the large-size box, B' is the large-size mass content in the large-size box. Here in this formulation r_K, r_B designates the input ratios of small and large-size mass contents in the total inflowing mass respectively; r'_K, r'_B symbolize the ratio of small-size to the total mass in the small box, ratio of large-size mass in the large-size box respectively; η_K, η_B signify small-size and large-size efficiency respectively.

Screen design

Design considerations

The theoretical model, so far developed, essentially couples the physical properties of the granular material with the characteristics of the mechanical environment. The basic physical properties in question are density and dimensions (width, length and thickness) of the grain; coefficients of friction between granular and screen and helicoid materials. The characteristics of the mechanical environment are fundamentally the shape and dimensions of the screen, namely cylinder radius and length, screen hole sizes (width and length), helix angle of helicoid; angular, axial and tangential velocities. The other quantities which go into the design procedure are the ones that depend on the interaction between granular material properties and screen characteristics. These are namely equilibrium angle, mass flowrate, limiting values of helix angle, axial and tangential velocities.

Another factor to be taken into consideration in describing the mechanical characteristics of the screen is the dimensions of the helicoid surface to be placed inside the cylinder surface of the screen. For all practical purposes, given the outer diameter of helicoid piece (*Dd*), pitch (h) and the width a, internal (*Di*'), and external (*Dd*') diameters of the planar ring that will form the helicoid were calculated as follows:

$$D'_d = \sqrt{D_d^2 + (h/\pi)^2}, D'_i = D'_d - 2a, D_d = 2r, h = 2\pi.r.tan\psi \tag{32}$$

The design procedure is to accept the desirable mass flowrate and physical properties of the granular material as the basic input and is to return the design quantities of the interest as the basic output.

Design algorithm

The mathematical model developed previously will be transformed into a number of series of consecutive steps to form an algorithm yielding the values of the design parameters. Series of steps are given below:

i. Desirable mass flowrate and the physical properties of the granular material are entered.
ii. The width of the oblong hole of the sheet metal is selected according to the classification table of granular material. For instance, the references (Guzel *et al.*, 2005, 2007; Akcali & Guven, 1990; Akcali *et al.*, 2006) are to be referred to when the granular material is peanut.
iii. Hole length is selected in relation to grain length.
iv. Taking into account the standards of sheet metal size, corresponding cylinder radius, length and thickness of sheet metal are chosen.
v. Limiting values of axial and tangential velocities are computed by (28) and (29) respectively.
vi. In order for the bulk not to stick on the internal surface of the cylinder angular speed should always be less than $w < \sqrt{\frac{g}{r}}$
vii. Tangential velocity of the granular material is computed by Eqn. (23).
viii. Tangential velocity is compared with its limiting value. If the limiting value is exceeded, the following actions are executed until satisfaction of the condition:
    a. Steps are iterated from vi.
    b. If action in step a is not sufficient, steps are iterated from iv.
ix. Helix angle is selected so as to satisfy inequality (21).
x. Axial velocity of the granular material is computed by Eqn. (22).
xi. Axial velocity is compared with its limiting value. If the limiting value is exceeded, steps are iterated from ix until satisfaction of the condition.
xii. Angle of equilibrium is found by an iteration technique using Eqn. (6) and initial solution (9).
xiii. Mass flowrate is calculated by means of Eqn. (21) and the relevant data.
xiv. Mass flowrate is compared with its desirable value. Until the desirable mass flowrate is satisfied with allowable tolerance, the following steps are iterated:
    a. Steps starting from number ix are repeated.
    b. If the steps in the previous iteration (a) do not satisfy the basic mass flowrate criterion, steps starting from number vi are repeated.
    c. In case the mass flowrate criterion is not satisfied in the previous step (b), then iteration is started from number iv thereafter.
xv. Helicoid dimensions are determined by Eqn. set (32).

Sorting machine was manufactured according to the above-mentioned design algorithm. The machine is shown in the Fig. 6. The basic feature of the machine is to allow different agricultural granular materials to be sorted out by the possibility of changing the cylindrical screen according to the fitting size of the granular material. In this particular machine, screen is intended to separate granular materials into two parts with diameter less or greater than 7 mm (Table 1). The dimensions and technical data, which belong to the cylindrical helical sieve, are presented in Table 1.

Limit and experimental speed values for the product to be moved on the sieve were calculated and given in Table 2. An examination of expressions (28) and (29) reveals that the limiting axial velocity (v_z) and tangential velocity (v_θ) are proportional with the dimensions of sieve hole along the axial and tangential directions, respectively. Axial hole dimension (*i.e.* hole length l_b) can be more freely selected whereas tangential hole dimension (*i.e.* hole width la) is dependent on the size of the granular material.

Figure 6. Helical screen

Table 1. The dimensions and technical data of the helical screen

Cylinder radius (r)	0.318 m
Cylinder length	1 m
Sheet metal thickness (c)	1.5 mm
Hole width (l_a)	7 mm
Hole length (l_b)	13 mm
Rotation speed	9.8 rpm
Helix angle	12°
Electrical motor power	0.36 kW

Table 2. Limit and experimental speeds on the sieve

Speeds	Limit	Experimental
Axial speed (v_z), m/s	0.176	0.069
Tangential speed (v_θ), m/s	0.327	0.326

When the thickness of the screen metal (c) and thickness of the granular material (e) are increased, both velocity limits are decreased at the same time.

Machine experiments

The parts that make up the prototype sorting machine are generally as follows: store (1), feeder outlet (2), transport channel (3), cylindrical sieve (4), helical paths (5), large kernels output (6), small kernels output (7), electrical motor (8), belt pulley mechanism (9) and brush (10). At the outlet (2) of the feeder there is a gate controlling the amount of particulate material fed into system, which is driven by a cylindrical cam mechanism at a frequency four times that of the cylinder (4). The system is activated by an electrical motor (8) through a belt and pulley mechanism (9). The machine functions in such a way that upon activation, the outlet (2) of the feeder store (1) filled with large and small sized kernels, forwards the particulate material through the transport channel (3) into the inlet part of the cylindrical screen (4). To prevent oblong holes on the screen from being blocked by kernels, a brush (10) extending along the cylinder is placed (Fig. 1b). In order to secure single and continuous layer, three helical paths (triple helicoid) have been deployed inside the cylinder.

Experiments on the machine are carried out in the following way: nine different large and small peanut mixtures (10-90%, 20-80%, 30-70%, 40-60%, 50-50%, 60-40%, 70-30%, 80-20% and 90-10%) were prepared with a total mass of 2 kg. Each mixture was filled into the store (1) at the back of the machine and the separation work was done by operating the machine. This process was repeated three times. The feeder outlet (2) was kept at the lowest level in order to enable the kernels to form a single layer in the cylinder. In the separation work, small sized peanuts fall down through the holes on the cylindrical screen (4) and are taken out from the small kernels outlet (7). The large kernels move along the cylinder and leave the machine from the large kernels outlet (6) at the end of the cylinder. Kernels from the outlets (6 and 7) were weighed on a sensitive scale with 1 g resolution and the resulting efficiencies of the mixture were determined.

The data were processed with the Excel 2016 package program. ANOVA was performed to determine the effect of large-small kernel mixture ratio on sorting success (SPSS v17.0).

Results

Experiments have been carried out on the manufactured machine to separate peanut kernels into small-size part with diameter less than 7 mm and large size part greater than 7 mm. The purposes of the experiments have been to determine efficiency (η), sensitivity of the size on the efficiency and to compare theoretical and experimental results.

The ratios of small-size (r_K), large-size (r_B) peanuts have been taken as 90-10%, 80-20%, 70-30%, 60-40%, 50-50%, 40-60%, 30-70%, 20-80% and 10-90% in the experiments. The resulting quantities in the small box and large box have been shown in Table 3. By using the experimental data in Eqn. 30 and 31 system efficiencies have been calculated and the results are displayed in last column of Table 3. Results indicate that the efficiency of the machine is independent of small-size ratio and hence quite satisfactory. The effect of the mixing ratio on the sorting efficiency was found to be statistically insignificant (p> 0.05).

Table 3. Experimental results

Exp. Mode	Input		Output in boxes		Efficiency (%)
	Small-size (g)	Large-size (g)	Small-size (g)	Large-size (g)	
A	1800	200	1795	205	99.4
B	1600	400	1592	408	99.5
C	1400	600	1398	602	99.8
D	1200	800	1196	804	99.6
E	1000	1000	996	1004	99.6
F	800	1200	798	1202	99.8
G	600	1400	595	1405	99.5
H	400	1600	396	1603	99.2
I	200	1800	196	1804	99.5

In order to determine experimental values of axial and tangential velocities, time elapsed corresponding to the displacement of cylinder length and angular velocity of the cylinder were measured as 14.5 s and 9.8 rpm, respectively. The average material thickness, after measurements in the sample, has been determined to be 6.24±0.53 mm. Accordingly, the theoretical developments associated with the screening conditions, namely satisfaction of limitations on axial and tangential velocities shown in Table 2 have also been justified by the experimental results.

Since equilibrium angle (β) has impact on the comparison of the important theoretical and experimental quantities, equilibrium angle (β) has been selected as the basis of this comparison. The theoretical value of β angle has been estimated by plotting F(β) under the values given in Table 1 and the coefficient of friction (μ) being taken as 0.35, which is determined from experiment (inclined plane method). The value at which the function F(β) changes sign has been determined as the theoretical β angle. On the other hand, the value of β experimental angle has been found by measuring the relevant angle in a predetermined circular plane under steady state conditions (Fig. 7).

The theoretical beta angle was calculated as 39.5 degrees (Eqn. 6). However, the beta angle obtained during the tests was measured around 40 degrees. There are 0.5 degrees difference. The difference is attributed to the variations in the coefficient of friction, which arises from discontinuous sheet metal surface full of oblong shaped holes.

Discussion

Using vibration in sieving and sorting is a known method and used since ancient times. As is also known, the vibration mechanism has drawbacks and creates noise, especially in fast operation (Chathurangani *et al.*, 2012). Alternatively, rotating cylindrical screens are used. For the material flow, these roller screens are operated inclined (Quaye & Schertz, 1983). However, flow smoothness is problematic. In the cylindrical sieve used in this study, a smooth material flow is provided by placing helicoid surfaces. The theory of a screening machine to separate the peanut seeds into two different classes has been developed, thus making it possible to manufacture the machine by which experiments have been carried out accordingly. By the experiments efficiency has been determined. The effect of grain size on the separation efficiency has been studied and theoretical and experimental equilibrium angles were determined and compared with each other. The separation efficiency of the machine (99% and above) has been found to be very good. The separation efficiency of the machine has not been affected by the small size ratio in the mixture. The limitations of theoretical velocities (axial, 0.176 m s^{-1} and tangential, 0.327 m s^{-1}) of a seed motion on the cylindrical sieve surface were consistent with those obtained experimentally (0.069 and 0.326 m s^{-1}). No significant difference has been observed between the theoretical and experimental values of equilibrium angle. It has been discovered in this study that this machine has done a perfect separation function. Experiments and observations made on this machine imply that prospects are high about the point that this machine can be utilized for other agricultural particulate materials with smooth surfaces such as soybeans, kidney beans, peas etc.

The relation between the theory and experiments has been of outmost importance in this work. Within this context, one important implication of the experiments is that the view that the regulation of motion is crucial to the achievement of high efficiency in the machine has been verified by the experiments. To secure this result, practical means such as feeder outlet facility making adjustments possible in the flowrate into the cylinder, multiple helicoids, brushes, satisfying theoretical assumptions have had to be deployed. The fact that the screening conditions made it foremost necessary to limit the two (tangential and axial) velocities has caused the operational angular speed of the rotating cylinder to be restricted. Additionally, in order to obtain a single layer in the machine, another assumption of the theory, the amount of material to be fed into the cylinder has had to be regulated by means of adjustments on the outlet of the feeder. Furthermore, the blockage of the holes has been prevented by using brushes at suitable locations, where the screening action is not executed. The use of 2 kg samples in the experiments has also been mandatory for the same reasons, namely that all the peanut items have had to be measured one by one to make sure that the ratios of small and large sized items comply with those planned in the experiments. From these explanations, it is evident that the flowrate has not been prioritized in these experiments. This point is of importance for future work, where flowrate formulation is not to depend on single-layer theory but rather on multi-layer theory together with some possible semi-empirical relations coming from the interaction of the particulate material with the manufactured model of the machine.

Figure 7. Estimation of experimental β angle.

A quantitative comparison can be made between the vibrationless rotating screen and traditional flat screen systems under similar conditions. One striking difference between them is that vibrationless sorting system has 99% and above efficiency, whereas the traditional flat screen has a base efficiency of around 85% (James & Sullivan, 2013). The comparison would be better understood if with the same perforated sheet used in the manufacturing of the vibrationless rotating screen, which is of 1x2 m dimensions, were to be utilized in the traditional flat screen to set similar conditions. First of all, the area (2 m^2) required by the traditional flat screen in the production site would be 3.14 times more than that of the cylindrical screen of this work, which occupies only an area of 0.636 m^2. Due to the fact that the structure of vibrationless rotating screen imposes onto the system two-fold restrictions on rotational speed, in tangential and axial directions within the context of regulated motion, its angular speed (9.8 rpm) is far less than that of the traditional flat screen, which is between 190 rpm and 380 rpm according to a study of Akcali & Mutlu (1992). Accordingly, considering only the velocity component required in the power computation, the power consumption based only on velocities would be on the average less than 5% in vibrationless rotating screen relative to that of the traditional flat screen. The energy needed in the vibrationless rotating screen under steady-state conditions is dissipated only to raise the center of mass of the layer to an equilibrium height, whereas the energy for the flat screen is mostly dissipated to overcome the large inertia of the sheet metal part because of the jerky motion. Moreover, it is probable that the inevitable jerky motion involved in the operation of the traditional flat screen will have a damaging effect on the crop seed quality especially when the seeds expected to possess germination ability are to be used for planting. From the standpoint of the amount of particulate material to be processed by the vibrationless rotating screen, it would be 1/9 times that of the traditional flat screen, since all the area (2 m^2) in the flat sheet will be covered by the particulate material while only an area of (2 m^2 × 400 / 360^0 = 0.222 m^2) of the cylindrical screen is covered in the case of vibrationless rotating screen. This point is worth of investigating in a future work, where multi-layer theory handling the flowrate issue of the vibrationless rotating screen has to be developed. Nevertheless, vibrationless rotating screen is believed to have significance in applications where high screening efficiency is sought, such as sensitive crop seed classification in procuring plant materials.

References

Akcali ID, Guven O, 1990. Physical properties of peanut in Turkey. Agricultural Mechanization in Asia, Africa and Latin America 3:55-60.

Akcali ID, Mutlu H, 1992. Analysis and design of a vibrating sieve. Proc 5th Nat Congr of Machine Design and Manufacturing, 16-18 Sept, METU, Ankara, pp: 229-240. (In Turkish).

Akcali ID, Ince A, Guzel E, 2006. Selected physical properties of peanuts. Int J Food Propert 9: 25-37. https://doi.org/10.1080/10942910500471636

Alkhaldi H, Eberhard P, 2006. Computation of screening phenomena in a vertical tumbling cylinder. Proc Appl Math Mechan, March 27-31, Berlin, 6 (1): 83-84. https://doi.org/10.1002/pamm.200610022

Chathurangani OS, Perera WJMK, Kumari HMNS, Subashi GHMJ, De Silva GSY, 2012. Utilization of sawdust and coconut coir fibre as noise reducing wall surface materials. Civil Eng Res Exchange Symp 2012, Matara, Sri Lanka, pp: 16-19.

Feistritzer WP, Vock H, Reiter H, 1981. Cereal and grain-legume seed processing. FAO Plant Prod Prot Series No. 21. Rome, Italy. 77 pp.

Fellows P, 2000. Food processing technology, 2nd ed. Cambridge, UK. 575 pp. https://doi.org/10.1201/NOE0849308871

Grandison AS, 2006. Postharvest handling and preparation of foods for processing. In: Food processing handbook; Brennan JG (Ed). Weinheim, Germany. pp: 1-30. https://doi.org/10.1002/9783527634361.ch1

Guzel E, Akcali ID, Mutlu H, Ince A, 2005. Research on fatigue behavior for peanut shelling. J Food Eng 3: 373-378. https://doi.org/10.1016/j.jfoodeng.2004.04.028

Guzel E, Akcali ID, Ince A, 2007. Behavior of peanut bulk under static loads. J Food Eng 5: 385-390. https://doi.org/10.1016/j.jfoodeng.2005.11.019

He X, Liu C, 2009. Dynamics and screening characteristics of a vibrating screen with variable elliptical trace. Mining Sci Technol 19: 0508-0513. https://doi.org/10.1016/S1674-5264(09)60095-8

Hongchang L, Yaoming L, 2011. Simulation and analysis of nonlinear motion for material particles on vibrating screen. IEEE Int Conf Publ on New Technol Agr Eng (ICAE) 5: 38-43.

James F, Sullivan PE, 2013. Screening theory and practice. Triple/S Dynamics, ebook, 50 pp.

Jiannan W, Huanxiong X, Zhichao H, Lianglong H, Baoliang P, Minji L, 2017. Parameter optimization on mechanical coating processing of rotary table-roller coating machine for peanut seeds. T Chin Soc Agr Eng 33 (7): 43-50.

Quaye SA, Schertz CE, 1983. Corncob harvest with counter-rotating rollers. T ASAE 26 (5): 1303-1307. https://doi.org/10.13031/2013.34120

Shen HP, Li J, Deng JM, Liu YW, Ding L, Zhang JT Zhang HF, Yang TL, 2009. A novel vibration sieve based on the parallel mechanism. IEEE 10th Int Conf

Publ on Comput Aided Indust Design & Concept Design 4: 2328-2332.

Stoicovici DI, Ungureanu M, Ungureanu N, Banica M, 2009. Computer model for sieves' vibrations analysis, using an algorithm based on the false-position method. Am J Appl Sci 6: 48-56. https://doi.org/10.3844/ajas.2009.48.56

Tan J, Harrison HP, 1987. Screening efficiency for planar and spatial drive mechanisms. Am Soc Agr Eng 30 (5): 1242-1253. https://doi.org/10.13031/2013.30552

Zhao L, Zhao Y, Liu C, Li J, Dong H, 2011. Simulation of the screening process on a circularly vibrating screen using 3D-Dem. Mining Sci Technol (China) 21: 677-680. https://doi.org/10.1016/j.mstc.2011.03.010